Int. J. Solids Structures, 1976, Vol. 12, pp. 693–703. Pergamon Press. Printed in Great Britain

A STUDY OF WAVE MOTION IN FIBER-REINFORCED MEDIUM

C. H. YEW and P. N. JOGI

Department of Aerospace Engineering and Engineering Mechanics, University of Texas at Austin, Austin, TX 78712, U.S.A.

(*Received* 10 *October* 1975; *revised* 26 *March* 1976)

Abstract—Measurements, both macroscopic and microscopic, of longitudinal wave motions propagating in the direction of reinforcing fibers were made on laboratory fabricated fiber-reinforced composites. Two waves with different propagation speeds and amplitudes were observed. Results are in good agreement with the predictions based on the mixture theory and the effective stiffness theory.

INTRODUCTION

During the last decade, the subject of wave motions in a fiber-reinforced composite has been extensively studied by many investigators. We cite here the analytical works by Sve[1, 2],† the "effective stiffness theory" by Achenbach, Sun and Herrmann[3–5] and the "mixture theory" by Bedford[6] and Hegemier[7–9]. Despite the differences in approach and methods, the same conclusion regarding the dispersive characteristics of waves in such a material has been reached by the above authors. Furthermore, analytical studies on the micro-motions in a composite have also been carried out in detail by these authors. The present investigation is closely related to the above analytical studies.

Experimental investigations on the dispersion of waves in a fiber-reinforced composite were carried out by Sutherland[10] and Tauchert[11]. The experimentally determined dispersion curves were in good agreement with the analytical predictions. Studies of the propagation of a transient pulse in a fiber-reinforced composite were carried out both analytically and experimentally by Peck[12], Whittier[13], and more recently by Sve[14]. In their experiments, one side of the specimen was subjected to an impulse generated in a shock tube, measurement of the surface velocity was made on the opposite side of the specimen by means of a capacitance probe. Since the capacitance probe has a finite probe surface, the measurements made by these authors are therefore the macroscopic motion in the specimen, i.e. an average velocity over the effective area of the probe. Good agreement between the measured results and analytical predictions was also reported.

In this paper, results from the experimental studies of wave motions, both macroscopic and microscopic, in a laboratory fabricated fiber-reinforced composite are presented. For the microscopic motion an optical interferometer[15] which is capable of making a point-wise measurement on the surface of the specimen was used to measure the motion of a fiber and the motion of a point on the matrix surface. For the macroscopic motion, a piezo-electric transducer was used to monitor the average motion on the surface of the specimen. In the following sections, the specimen used in the investigation will first be described. It is then followed by a detailed description of the experimental arrangement and method. To facilitate the interpretation of the experimental results, wave analyses based on the mixture theory[8] and a simplified effective stiffness theory[16] are carried out in section three. The comparison and discussion of the experimental findings with the predictions from these two theories are presented in the conclusion of the paper.

DESCRIPTION OF SPECIMEN

The specimens used by Sve[14] were made of alternating layers of thin plastic and metallic sheets (the approximate thickness of each sheet was 0.762 mm) bonded together by a special type of adhesive. Sutherland[10] used an aluminum-tungsten composite in his experiment. The specimen was fabricated by embedding 0.127 mm dia. tungsten wires in an aluminum matrix by

†Numbers in the bracket designate the references at the end of paper.

means of the tape lamination technique. The specimens adopted by the above investigators were, however, not suitable for the present investigation. Since the purpose of this investigation was to study the micro- and macro-motion of the constituents of the composite material, very thin fibers or laminates and very dense fiber geometry would make an accurate and meaningful micro-motion measurement on an individual component (say fiber of the specimen) very difficult. In view of this, a specially designed specimen was fabricated for this investigation.

The fiber-reinforced specimens used in this investigation were made of plastic material reinforced by parallel steel wires. The matrix plastic material is a photoelastic sensitive material known as PLM-4 supplied by the Photolastic Company[18]. The steel wires were first straightened and then carefully installed into a mold of hexagonal geometry. The liquid plastic was then cast into this mold. After solidification, the fiber reinforced plastic was removed from the mold, machined and polished to the desired dimensions. The residual stress in the specimen due to casting and machining was checked by a polariscope, and if present was removed by repeated annealling and polishing. A thin layer (approximate thickness = 6 Å) of silver was afterwards vapor-deposited on one surface of the specimen for reflecting the light beam from the optical interferometer. A photograph of a representative specimen is shown in Fig. 1. The geometrical description of specimens used in this investigation and the material properties of fiber and matrix material are tabulated in Table 1. It should be mentioned here that the material properties of PLM-4 epoxy presented in Table 1 were experimentally verified by measuring the shear and dilatational wave speeds in this material. Finally, the dispersion curves of a representative specimen A-4 calculated from the mixture theory[8] and the effective stiffness theory[16] are depicted in Fig. 2. To facilitate the discussion, the numerical presentations in the subsequent sections will be based on the data from this specimen.

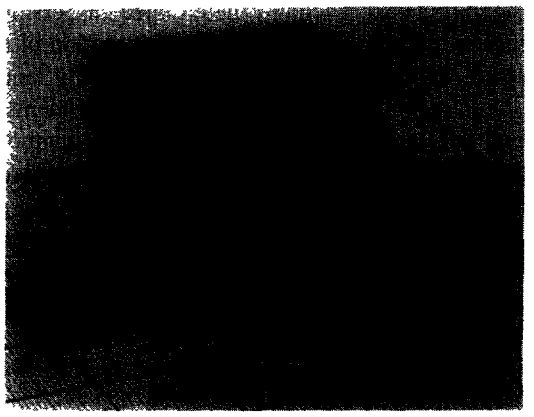

Fig. 1. A-4 specimen.

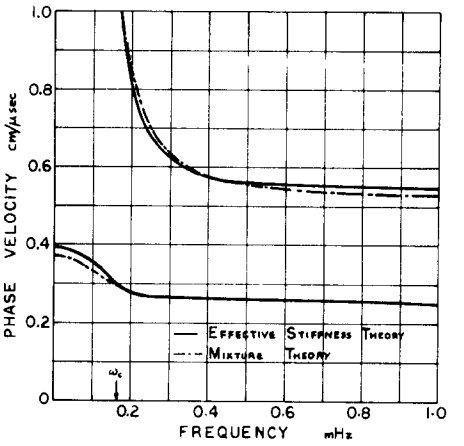

Fig. 2. Dispersion curves of A-4 specimen.

EXPERIMENTAL ARRANGEMENT

In view of the dispersion curves shown in Fig. 2, it becomes apparent that for a meaningful study of the wave motions in this specimen, the testing frequency range should be broad enough to include the cut-off frequency ω_c. To satisfy this requirement, the test frequency in this investigation ranged from 50 kHz to 1.5 mHz.

The experimental arrangement for the macroscopic motion studies is sketched in Fig. 3. It is similar to that used by Tauchert[11]. Two identical x-cut Lead Zirconate Titanate disks (1″ in dia., ± 5% in resonant frequency) are placed on the central portion of the opposite sides of the specimen. One disk serves as the driver and the other serves as the receiver. A repeated wave pulse of eight or more cycles at a given frequency was tone-bursted into the specimen by the driving disk. The period between the wave pulses was kept long enough for the motion in the specimen to be damped out before the arrival of the next pulse. As the transmitted wave pulse arrives on the other side of the specimen, it is sensed by the receiving disk. Figure 4 shows the oscilloscope pictures of a clear specimen (no reinforcing fiber) tested at a frequency of 1.1 mHz

Table 1. Specimen geometry and material properties

Specimen no.	Thickness cm	Fiber Dia cm	Fiber Spacing cm	Mixture Theory v_1 cm/μsec	Mixture Theory v_2 cm/μsec	Effective Stiffness Theory v_1 cm/μsec	Effective Stiffness Theory v_2 cm/μsec	Measured Wave Speed v_1 cm/μsec	Measured Wave Speed v_2 cm/μsec
A-1	3.856	0.16	0.32	0.52	0.249	.574	.249	0.54	0.23
A-2	3.974	0.16	0.4	0.518	0.248	.564	.249	0.55	0.24
A-3	3.848	0.16	0.48	0.518	0.249	.554	.249	0.55	0.25
A-4	4.08	0.16	0.56	0.514	0.248	.543	.249	0.56	0.25
B-1	0.927	0.0762	0.1524	0.520	0.248	.574	.249	0.51	0.23
B-2	0.937	0.0762	0.1905	0.518	0.249	.564	.249	0.49	0.23
B-3	1.176	0.0762	0.2286	0.518	0.248	.554	.249	0.49	0.23
B-4	1.176	0.0762	0.3048	0.516	0.249	.543	.249	0.49	0.23

Properties	Steel Fiber	PLM-4 Liquid Epoxy Resin
Density (gm/cm^3)	7.8	1.23
Shear Modulus μ(dynes/cm^2)	8.1×10^{11}	16.88×10^9
Lame Constant λ(dynes/cm^2)	11.2×10^{11}	42.5×10^9
E (dynes/cm^2)	21×10^{11}	44.9×10^9
Poissons Ratio ν	0.29	0.36
Velocity (met./sec.) (dilitational)	5940	2492
Velocity (met./sec.) (shear)	3220	1171

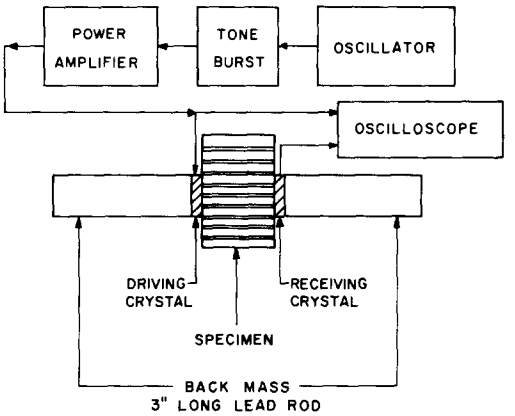

Fig. 3. Schematic diagram of experimental arrangement for macro-motion measurement.

and a fiber-reinforced specimen tested at 58 kHz, 377 kHz, 764 kHz and 1.047 mHz. The arrival time of the wave pulse was determined directly from the oscilloscope picture. The wave speed was then determined by dividing the specimen thickness with the transit time. During the experiment, the wave speed was frequently checked with an aluminum block of constant thickness to ensure the proper functioning of the testing apparatus.

Since the output signal of the crystal depends upon the average movement of its contact surface with the specimen, the information obtained by this means may be regarded as macroscopic. It should be mentioned here that this method provides accurate information concerning the arrival times of the waves, but it does not however, provide any accurate information on the wave amplitude. The capacitance probe used by Whittier[13] Sve[14] would be a sensor for both velocity and displacement measurement. However, the amplitude of waves in the present arrangement proved to be too small to be measured by a capacitance probe.

The photographs in Fig. 4 clearly exhibit the wave characteristics in a fiber-reinforced specimen. For frequencies higher than $\omega_c = 0.168$ mHz, there are two wave fronts as shown in Figs. 4-2, 4-3 and 4-4; the wave speeds of these two fronts were found to be nearly constant at all frequencies. A tabulation of these two wave speeds for all the specimens is presented in Table 1. The significance of this finding will be discussed in detail in later sections.

An optical interferometer[15] was used for the measurement of the micromotion in the

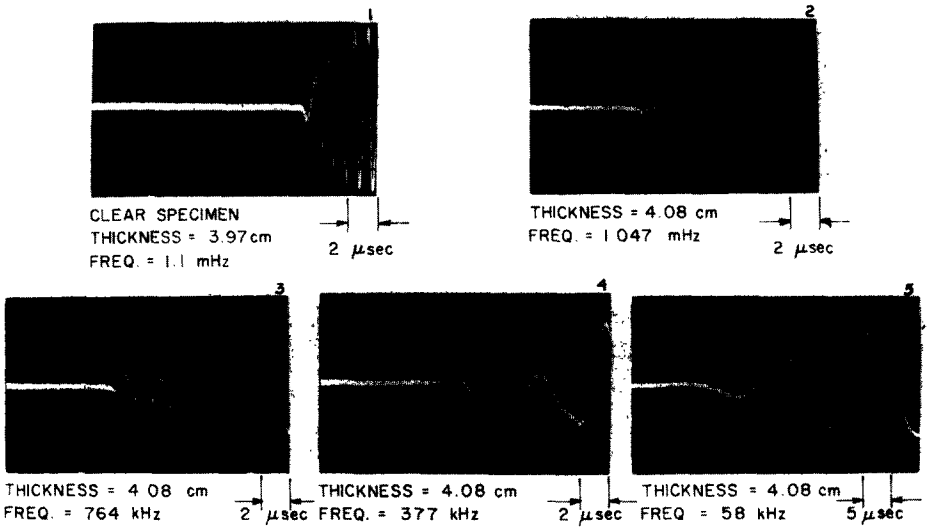

Fig. 4. Macro-motions in A-4 specimen.

specimen. A schematic diagram of the optical arrangement is shown in Fig. 5. Using this arrangement, it is possible to focus the sensing light beam on a point (small area) on the end surface of a fiber or on a point on the matrix surface. In this investigation, measurements of fiber and matrix movement were made on the central portion of the specimen. A photomultiplier tube (EMI 9558B) with adequate frequency response was used to sense the optical fringe change resulting from movement of the specimen surface. Figures 6a and 6b show the oscilloscope records of the photomultiplier output of the matrix motion and the fiber motion of the specimen tested at various frequencies. For the purpose of illustration, the photomultiplier output from a clear specimen (with no reinforcing fibers) tested at 521 kHz is also shown in Fig. 6a. Since the output of the photomultiplier is frequency modulated (i.e. one complete oscillation represents one wave length of the laser light ($\lambda = 6280$ Å) change of displacement), the wave amplitude in the clear specimen is more that one λ. The reverberation of the wave inside the specimen is clearly demonstrated in this photograph.

The amplitude of the input wave is estimated by the formula†

$$U_{in} = \frac{1}{2}[d_{33}V] \tag{1}$$

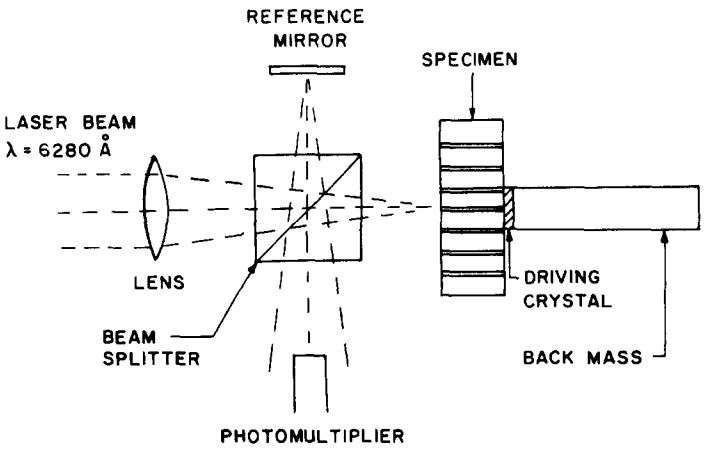

Fig. 5. Optical arrangement of the interferometer.

†A discussion of this equation is presented in a later section.

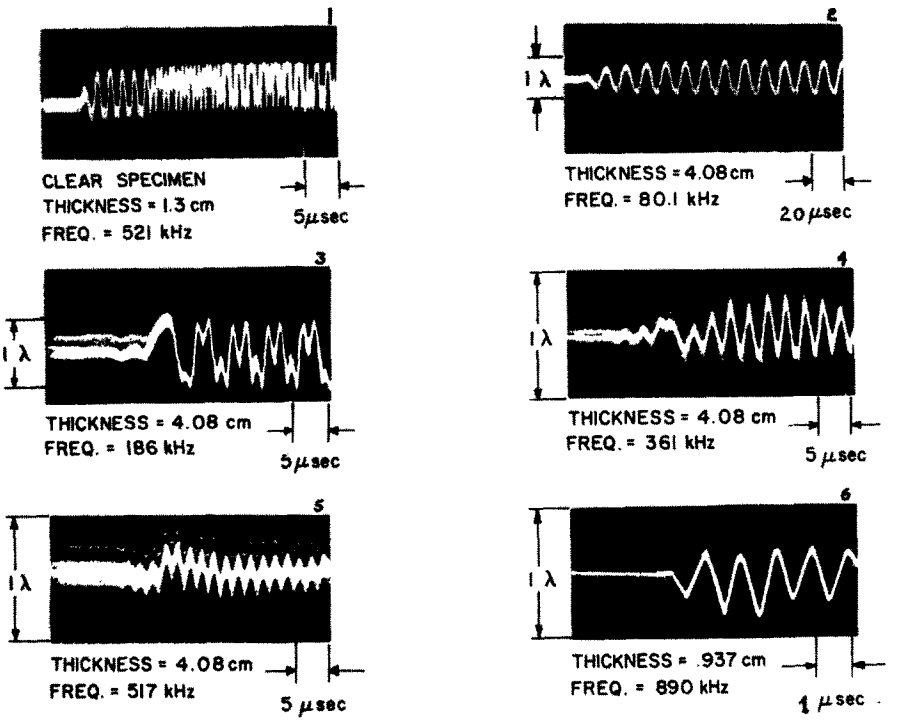

Fig. 6a. Displacement-time records of a point on the matrix surface of specimen.

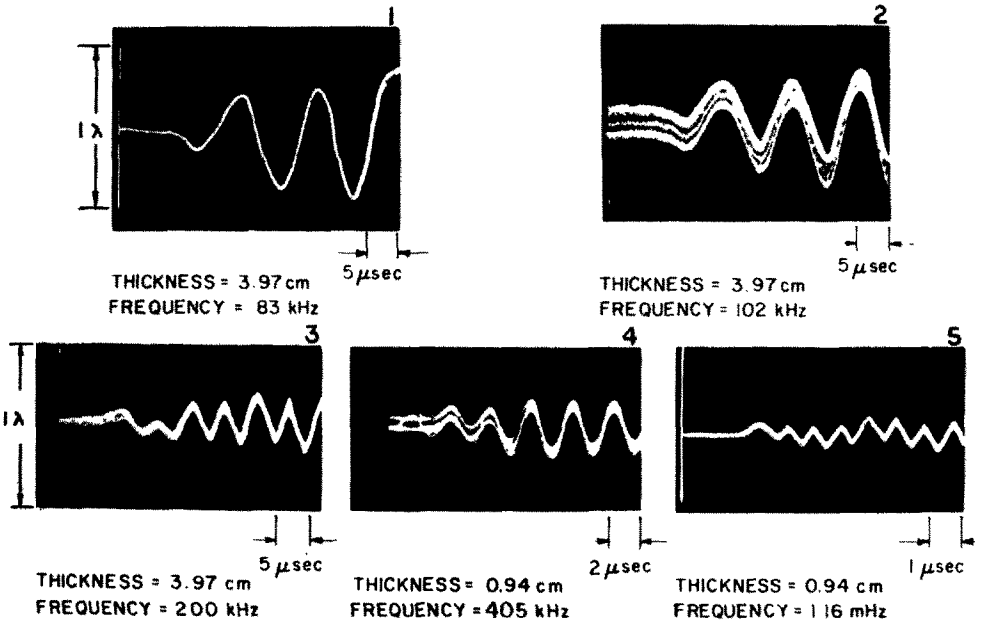

Fig. 6b. Displacement-time records of the motion of a fiber.

where d_{33} is the piezo-electric charge coefficient ($d_{33} = 280 \times 10^{-12}$ meter/meter per volt/meter of disk thickness) of the disk and V is the voltage applied to the piezo-electric disk. To facilitate the interpretation of data, the output wave amplitude was limited below one λ† in all the experiments. The amplitude of oscillation of the specimen shown in Fig. 6 can therefore be determined directly from the picture using a calibration equation

†For frequencies higher than 700 kHz, we were unable to generate an amplitude greater than one λ.

$$U_{out} = \frac{2h}{H}\lambda \tag{2}$$

where h is the measured amplitude and H is the calibration length as shown in the beginning of each trace in Figs. 6a and 6b.

Figures 6a-2 and 6a-6 show a single wave but with different propagating speeds. Figures 6a-3, 6a-4 and 6a-5 show two waves with different propagating speeds and amplitudes. Note also that the amplitude of the second wave in Fig. 6a-2 is slightly larger than one λ. The measured wave speeds were found consistent with those found in the macro-motion measurement. Denoting the waves according to their arrival sequence as the 1st and 2nd waves, the amplitude–frequency relationships of these waves are plotted with the analytical predictions in Fig. 7. Again the discussion of these results is deferred to a later section.

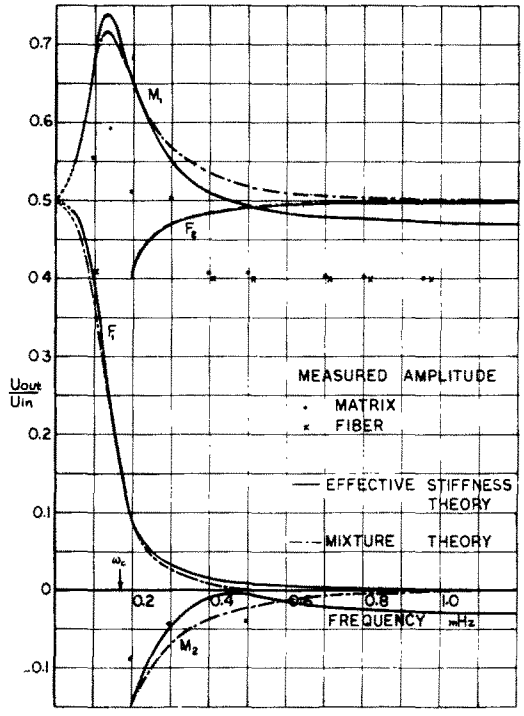

Fig. 7. Amplitude ratio vs frequency of a point on the surface of specimen.

ANALYSIS OF WAVE MOTIONS

Prior to analyzing and discussing the experimental results, it is advantageous to briefly summarize the wave behavior in a fiber-reinforced composite predicted by the existing theories. Based on the "effective stiffness" theory the problem of propagation of a step pressure pulse in such a medium was studied by Sve[17] using the "head-of-the-pulse" technique. Sve found that when the direction of the impulse is in line with the fiber, a single pulse with small oscillations superimposed on the main body of the pulse propagates through the composite with a constant velocity. Applying the same technique, similar results were obtained by Martin[19] based on the "mixture theory." The analytical predictions were found in good agreement with the experimental results obtained by Whittier[13] and Sve[14].

Since the head-of-the-pulse method is accurate only for long times, and since the geometrical configuration of the specimen used in this investigation is different from that used by Whittier and Sve, it becomes necessary to reexamine the wave equations in a manner consistent with the present experimental arrangement. For this purpose, analyses of wave motions in a fiber-reinforced composite based on the mixture theory[8] and on the simplified effective stiffness theory[16] are presented in the following sections:

(a) *Wave motions based on the mixture theory* [8]†

Based on this theory, the equations of motion have the form

$$c_{11}\frac{\partial^2 u_f}{\partial x^2}+c_{12}\frac{\partial^2 u_m}{\partial x^2}-\rho_f\frac{\partial^2 u_f}{\partial t^2}=K^*(u_f-u_m)$$

$$c_{12}\frac{\partial^2 u_f}{\partial x^2}+c_{22}\frac{\partial^2 u_m}{\partial x^2}-\rho_m\frac{\partial^2 u_m}{\partial t^2}=-K^*(u_f-u_m) \tag{3}$$

where u_f and u_m are the displacement of the reinforcing fiber and the matrix material respectively and K^* is the coupling parameter. It should be pointed out here that eqn (3) is identical to the equation derived by Bedford[6]. Since the elastic modulus of the piezo-electric disk ($E = 9.7\times 10^6$ psi) used in this study is much higher than the modulus of the matrix material, the boundary condition on the forcing side of the specimen can be written as

$$u_f(0,t)=u_m(0,t)=U_{\text{in}}\sin\omega t[H(t)-H(t-T)] \tag{4}$$

where U_{in} is the amplitude of oscillation, ω is the angular frequency, $H(t)$ is the Heaviside step function, and T is the time duration of the pulse. For mathematical simplicity, the specimen is regarded as a semi-infinite medium. This assumption does not satisfy the actual test condition. However, since only the transient wave is of the main interest here, the assumption of a semi-infinite medium would be justifiable as long as the arrival of waves is not affected by the reflected waves from the boundaries of the specimen.

Assuming that the medium is initially at rest, the Laplace transformation of eqns (3) and (4), after some algebraic manipulations, gives the expression for the matrix displacement as

$$U_m=\frac{U_{\text{in}}\omega}{2\pi i}\left[\int_{B_r}\frac{(1-e^{-Ts})(s^2b-\lambda_2^2)}{(s^2+\omega^2)(\lambda_1^2-\lambda_2^2)}e^{-\lambda_1 x+st}\,ds-\int_{B_r}\frac{(1-e^{-Ts})(s^2b-\lambda_1^2)}{(s^2+\omega^2)(\lambda_1^2-\lambda_2^2)}e^{-\lambda_2 x+st}\,ds\right] \tag{5}$$

A similar expression for the fiber displacement is not repeated here. Here s is the Laplace parameter and the constant b, expressed in terms of the constants in Ref. [8], may be written as

$$b=\frac{c_1^2-c_{12}/\rho_2}{c_1^2c_2^2-c_3^4} \tag{6}$$

The parameters

$$\lambda_{1,2}^2=\frac{1}{2(c_1^2c_2^2-c_3^4)}[\nu c_0^2+s^2(c_1^2+c_2^2)\pm\sqrt{([\nu c_0^2+s^2(c_1^2+c_2^2)]^2-4s^2(s^2+\nu^2)(c_1^2c_2^2-c_3^4))}] \tag{7}$$

are the roots of the equation

$$(c_3^4-c_1^2c_2^2)\lambda^4+[\nu c_0^2+s^2(c_1^2+c_2^2)]\lambda^2-(\nu s^2+s^4)=0. \tag{8}$$

We note that eqn (8) becomes the dispersion relation derived by Hegemier[8] when the Laplace parameter s is replaced by $i\omega$. Invoking the condition of real wave speeds ($\lambda_{1,2}$), the cut-off frequency ω_c can be calculated.

A suitable contour for evaluating the integrals in eqn (5) is depicted in Fig. 8. In the following discussions, the integral was evaluated numerically based on the material constants of the representative specimen A-4 shown in Table 1. Equation (5) obviously suggests the existence of two waves in accordance with parameters λ_1 and λ_2. By evaluating the contour enclosed by the

†The notations used here are consistent with those used in Ref. [8].

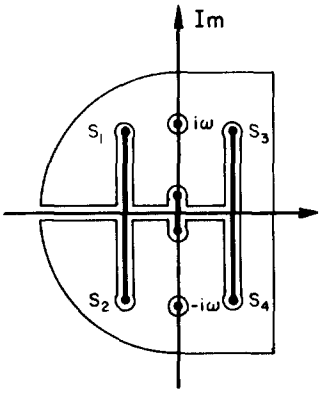

Fig. 8. Integration contour of eqn (5).

large semi-circle on the right half-plane, and making use of the Jordan's lemma, the wave speeds can be expressed as

$$v_{1,2} = \left[\frac{2(c_1^2 c_2^2 - c_3^4)}{c_1^2 + c_2^2 \mp \sqrt{((c_1^2 - c_2^2)^2 + 4c_3^4)}}\right]^{1/2} \tag{9}$$

The propagation speeds of these two waves depend upon the material properties of the fiber and the matrix and the fiber geometry. They are independent of the angular frequency of the wave.

The poles $s = \pm i\omega$, contribute to the steady-state solution of eqn (5). After considerable computations, the results may be summarized as follows: Corresponding to λ_1 and λ_2, the two waves are found to propagate with speeds $v_1 = 0.514\ \text{cm}/\mu\ \text{sec}$, and $v_2 = 0.248\ \text{cm}/\mu\ \text{sec}$. Both waves have the form

$$\left|\begin{matrix} u_l^m \\ u_l^f \end{matrix}\right| = \left|\begin{matrix} M_l \\ F_l \end{matrix}\right| e^{ik_l(x - c_l t)} \tag{10}$$

where $l = 1, 2$ implies the corresponding contribution from the parameters λ_1 and λ_2, and M_l and F_l are the amplitude of the matrix and the fiber waves respectively.

The amplitudes M_l and F_l are frequency dependent. They are plotted versus the frequency in Fig. 7 for $l = 1$ and 2 respectively. The relationship between the phase velocity c_l and the frequency is consistent with that shown in Fig. 2. The cut-off frequency is $\omega_c = 0.168$ mHz. Consequently the u_2-wave does not exist when the driving frequency is lower than ω_c.

Equating the expression $\lambda_1^2 - \lambda_2^2$ in the denominator of the integrand of eqn (5) to zero results in four branch points $s_{1,2} = \pm(-0.45 + 0.72\,i) \times 10^{16}$ and $s_{3,4} = \pm(0.45 + 0.72\,i) \times 10^6$. It can be shown that the contributions due to these branch points cancel each other due to their symmetrical properties. The parameters λ_1 and λ_2 in the exponentials of eqn (5) contribute three more branch points at $0, \pm 1.036 \times 10^6\,i$. Integration along the branch contour yields an integral of the same expression as the Love–Rayleigh integral. This integral contributes to the small oscillations superimposed on the main pulse as demonstrated by Hegemier[8] and Sve[17]. After considerable numerical manipulations, it can be shown that the contributions from this integral are three orders of magnitude smaller than the contributions from the poles $s = \pm i\omega$ in the present case.

(b) *Wave motions based on the effective stiffness theory* [16]

Consistent with the experimental arrangement, a simplified equation of motion for the wave motions in a fiber-reinforced specimen was recently developed by Achenbach[16] based on the effective stiffness theory. The equation has the form

$$L_1 \frac{\partial^2 u_f}{\partial t^2} + L_2 \frac{\partial^2 u_m}{\partial t^2} - L_3 \frac{\partial^2 u_f}{\partial x^2} - L_4 \frac{\partial^2 u_m}{\partial x^2} = 0$$

$$M_1 \frac{\partial^2 u_f}{\partial t^2} + M_2 \frac{\partial^2 u_m}{\partial t^2} - M_3 \frac{\partial^2 u_f}{\partial x^2} - M_4 \frac{\partial^2 u_m}{\partial x^2} + M_5(u_m - u_f) = 0 \tag{11}$$

where

$$L_1 = \bar{\rho} - \frac{b_1}{M}, \quad M_1 = b_1 - \frac{b_2}{M}, \quad M_5 = \frac{a_7}{M}$$

$$L_2 = \frac{b_1}{M}, \quad M_2 = \frac{b_2}{M}, \quad M = \sqrt{(\pi)}\, b \sin\left(\frac{\pi}{2}\frac{r-a}{b-a}\right)$$

$$L_3 = a_1 - \frac{a_5}{M}, \quad M_3 = a_5 - \frac{a_6}{M}$$

$$L_4 = \frac{a_5}{M}, \quad M_4 = \frac{a_7}{M}$$

$r = a$ is the radius of the fiber
$r = b$ is the radius of the unit cell

and

$$\begin{aligned}
a_1 &= \eta[\lambda_f + 2\mu_f] + (1-\eta)(\lambda_m + 2\mu_m) \\
a_5 &= \left[\frac{8}{\pi^2}(1-\eta^{1/2})^2 + \frac{4}{\pi}(1-\eta^{1/2})\right]\pi^{1/2} b(\lambda_m + 2\mu_m) \\
a_6 &= \left[\frac{8}{\pi^2}(1-\eta^{1/2})^2\left(\frac{\pi^2}{16}+\frac{1}{4}\right) + \eta^{1/2}(1-\eta^{1/2})\right]\pi b^2(\lambda_m + 2\mu_m) \\
a_7 &= \left[\frac{\pi}{2}\left(\frac{\pi^2}{4}-1\right) + \frac{\pi^3}{4}\eta^{1/2}\frac{1}{1-\eta^{1/2}}\right]\mu_m \\
b_1 &= \left[\frac{8}{\pi^2}(1-\eta^{1/2})^2 + \frac{4}{\pi}\eta^{1/2}(1-\eta^{1/2})\right]\pi^{1/2} b\rho_m \\
b_2 &= \left[\frac{8}{\pi^2}(1-\eta^{1/2})^2\left(\frac{\pi^2}{16}+\frac{1}{4}\right) + \eta^{1/2}(1-\eta^{1/2})\right]\pi b^2\rho_m
\end{aligned} \tag{12}$$

where η = volume density $= \dfrac{\text{Area of fiber}}{\text{Area of cell}}$

$\bar{\rho} = \eta\rho_f + (1-\eta)\rho_m$

Notations ρ_f and ρ_m refer to fiber and matrix densities respectively.

Following the same procedure as described in section (a), the matrix displacement can be expressed as

$$\begin{aligned}
U_m = \frac{U_{in}\omega}{2\pi i}\Bigg[&\int_{B_r} \frac{(1-e^{-Ts})(s^2\bar{b} - \lambda_2^2)}{(s^2+\omega^2)(\lambda_1^2 - \lambda_2^2)} e^{-\lambda_1 x + st}\, ds \\
&- \int_{B_r} \frac{(1-e^{-Ts})(s^2\bar{b} - \lambda_1^2)}{(s^2+\omega^2)(\lambda_1^2 - \lambda_2^2)} e^{-\lambda_2 x + st}\, ds\Bigg]
\end{aligned} \tag{13}$$

where

$$\bar{b} = \frac{L_1M_3 - L_3M_1 + L_2M_3 - M_2L_3}{L_4M_3 - M_4L_3}$$

and λ_1 and λ_2 are the roots of equation

$$\begin{aligned}
\lambda^4 + &\left[\frac{s^2(L_1M_4 + L_3M_2 - L_2M_3 - L_4M_1) + M_5(L_3 + L_4)}{M_3L_4 - L_3M_4}\right]\lambda^2 \\
&+ \left[\frac{s^4(L_2M_1 - L_1M_2) - s^2M_5(L_1 + L_2)}{M_3L_4 - L_3M_4}\right] = 0.
\end{aligned} \tag{14}$$

Equations (13) and (14) have the same form as eqns (5) and (8). Applying the same computational

procedure, the propagation speeds of the waves are found to be of the form

$$v_{1,2} = \left[\frac{2(a_1a_6 - a_5^2)}{(\bar{\rho}a_6 - 2a_5b_1 + a_1b_2) \mp \sqrt{((\bar{\rho}a_6 - 2a_5b_1 + a_1b_2)^2 + 4(b_1^2 - \bar{\rho}b_2)(a_1a_6 - a_5^2))}}\right]^{1/2}. \quad (15)$$

The dispersion curves computed from eqn (14), and the amplitudes M_i and F_i of the steady-state waves computed from eqn (13) are plotted in Fig. 2 and Fig. 7 respectively with the results computed from the mixture theory. The agreement is reasonably good.

DISCUSSION AND CONCLUSION

Based on the wave motion analysis presented in the previous section, it can be concluded that the main bodies of the wave are the two steady state waves due to poles $s = \pm i\omega$. These two waves propagate with a constant speed v_1 and v_2 depending upon the material properties and the fiber geometry of the composite.

The amplitude-frequency relationship of two waves based on the mixture and the effective stiffness theories are shown in Fig. 7. Wherein M_1, M_2, and F_1, F_2 are denoted as the amplitudes of two waves in the matrix and in the fiber respectively. In view of Fig. 7, the following experimental observation on the behavior of waves in the specimen may be expected.

(1) For $\omega < \omega_c$ (0.168 mHz), the micro-motion measurement should reveal a single wave, M_1 for the matrix and F_1 for the fiber. The macro-motion measurement should also reveal a single wave $M_1 + F_1$.

(2) For ω slightly higher than ω_c, the micro-motion measurement should reveal two waves in the matrix, M_1 and M_2, and two waves in the fiber, F_1 and F_2. The macro-motion measurement should also reveal two waves $F_1 + M_1$ and $F_2 + M_2$.

(3) For $\omega > \omega_c$, the micro-motion measurement should reveal a single wave in the matrix M_1, and a single wave in the fiber F_2. The macro-motion measurement should reveal two waves, M_1 and F_2.

The above conclusions are clearly supported by the experimental results shown in Fig. 4, Figs. 6a and 6b. Figure 4 shows a series of oscilloscope records of the macro-motion measurements. It clearly reveals the existence of two waves for frequencies higher than ω_c. The measured wave speeds are tabulated along with those calculated from both theories in Table 1. The agreement, although slightly in favor of the effective stiffness theory, is good with the predictions from both theories. It should be mentioned here that the arrival times of the waves were determined directly from the oscilloscopic records. An exact time is difficult to establish in this case, Based on the wave speed measurement on the standard aluminum block, the accuracy of the measured wave velocities is estimated to be within two percent. The relationship between the phase velocity c_i and frequency of these two waves establishes the dispersive characteristics of the waves as shown in Fig. 2. The experimental verification of these dispersion curves can only be achieved by phase angle measurement of the waves. This requires a precise frequency and wave form control. The accuracy of the frequency generator and power amplifier used in this investigation is $\pm 1\%$. Consequently, reliable phase angle measurements could not be made in this investigation.

The fiber and matrix motions for the micro-motion measurements are shown in Figs. 6a and 6b. In general, these motions agree with the analytical predictions. The wave speeds measured in this portion of the experiment agrees well with those determined from the macro-motion measurements. The amplitudes of waves show, however, some substantial discrepancies from the theoretical predictions. These discrepancies may be attributed to the following two reasons: (1) The displacement produced by the driving crystal disk is difficult to control and measure accurately. Equation (1) is only an approximate formula for estimating the displacement of the disk produced by the applied voltage. The exact calibration equation may be non-linear. It is well known that the actual displacement of the crystal disk depends upon not only the applied voltage but also the relative stiffness between the crystal disk and the specimen as well as the applied pressure and the frequency[20]. Consequently, the input displacement based on eqn (1) is not accurate especially at the high frequency range. (2) In order to separate these two expected waves, thick specimens were used in the investigation. Attenuation of waves introduces further errors in the final results. The results, nevertheless, display clearly the behavior of waves in the specimen.

The experimental results presented in this investigation suggest that both the mixture theory and the effective stiffness theory provide an excellent prediction on the behavior of longitudinal waves propagating in the direction of reinforcing fibers. In the case of a practical fiber-reinforced composite, the arrival times of these two waves are separated by only a fraction of a micro-second. Based on the constituent data of the quartz fiber-reinforced phenolic [8, 13, 14], the propagation speeds of these two waves are 0.3115 and 0.4238 cm/μsec respectively. Thus in a thin specimen, these two waves would be diffcult to separate in practice.

Acknowledgments—The authors wish to express their appreciation to Mr. W. Murto for his capable assistance in the experimental phase of this investigation, to Profs. E. A. Ripperger and A. Bedford for their valuable comments and suggestions during the course of investigation, and to Prof. J. D. Achenbach for providing the equations of motion based on the effective stiffness theory and his constructive comments on the original manuscript. This work is financially supported by the National Science Foundation (GK 39921).

REFERENCES

1. C. Sve, Time-harmonic waves traveling obliquely in a periodically laminated medium. *J. Appl. Mech.* **36**, 778–782 (1970).
2. C. Sve, Stress wave attenuation in composite materials. *J. Appl. Mech.* **39**, 1151–1153 (1972).
3. C. T. Sun, J. D. Achenbach and G. Herrmann, Continuum theory for a laminated medium. *J. Appl. Mech.* **35**, 467–475 (1967).
4. J. D. Achenbach and G. Herrmann, Effective theory for a laminated composite. *Developments in Mechanics*, Proc. 10th Midwestern Mechanics Conference, Colorado State University, Fort Collins, Colorado, pp. 91–106 (1968).
5. J. D. Achenbach, C. T. Sun and G. Herrmann, On the vibrations of a laminated body. *J. Appl. Mech.* **35**, 689 (1968).
6. A. Bedford and M. Stern, Toward a diffusing continuum theory of composite materials. *J. Appl. Mech.* **38**, 8–14 (1971).
7. G. A. Hegemier, On a thory of interacting continua for wave propagation in composites. *Dynamics of Composite Materials*. (Edited by E. H. Lee) pp. 70–121. ASME publication (1972).
8. G. A. Hegemier, G. A. Gurtman and A. H. Nayfeh, A continuum mixture theory of wave propagation in laminated and fiber reinforced composites. *Int. J. Solids Structures* **9**, 395–414 (1973).
9. G. A. Hegemier and I. C. Bache, A continuum theory for wave propagation in laminated composites—Case 2: propagation parallel to the laminates. *J. Elasticity* **3**, 125–140 (1973).
10. H. J. Sutherland and R. Lingle, Geometrical dispersion of acoustic waves by a fibrous composite. *J. Composite Materials* **6**, 490–502 (1972).
11. T. R. Tauchert and A. N. Guzelsu, An experimental study of dispersion of stress waves in a fiber-reinforced composite. *J. Appl. Mech.* **39**, 98–102 (1972).
12. J. C. Peck and G. A. Gurtman, Dispersive pulse propagation parallel to the interfaces of a laminated composite. *J. Appl. Mech.* **36**, 479–484 (1969).
13. J. S. Whittier and J. C. Peck, Experiments on dispersive pulse propagation in laminated composites and comparison with theory. *J. Appl. Mech.* **36**, 485–490 (1969).
14. C. Sve and S. Okubo, Experiments on pulse propagation in an obliquely laminated composite. *J. Appl. Mech.* 1052–1056 (1974).
15. M. A. Monahan and K. Bromley, Vibration analysis by holographic and conventional interferometry. NECL Report No. 1513, Naval Electronics Laboratory for Command Control and Communications (Sept. 1967).
16. J. D. Achenbach, Generalized continuum theories for directionally reinforced solid. *Archiwum Mechaniki Stosowanej.* To be published. Equation (11) was furnished by Prof. Achenbach through a private communication.
17. C. Sve and J. S. Whittier, One-dimensional pulse propagation in an obliquely laminated half space. *J. Appl. Mech.* 778–782 (1970).
18. *Instructions for Making Photoelastic Models.* Photolastic Inc., 67 Lincoln Hwy., Malvern, Pa., U.S.A.
19. S. E. Martin, A. Bedford and M. Stern, Steady state wave propagation in fiber reinforced elastic materials. *Developments in Mechanics*, Vol. 6, pp. 515–528. Proc. of the 12th Midwestern Mechanics Conference (1973).
20. W. P. Mason, *Piezoelectric Crystals and their Applications to Ultrasonics.* Van Nostrand, New York (1950).